Fingers-Closing and Other Rapid Conformational Changes in DNA Polymerase I (Klenow Fragment) and Their Role in Nucleotide Selectivity[†]

Catherine M. Joyce,* Olga Potapova, Angela M. DeLucia,[‡] Xuanwei Huang,[§] Vandana Purohit Basu, and Nigel D. F. Grindley

Department of Molecular Biophysics and Biochemistry, Yale University, New Haven, Connecticut 06520

Received November 1, 2007; Revised Manuscript Received February 16, 2008

ABSTRACT: We have developed a FRET-based assay for the fingers-closing conformational transition that occurs when a binary complex of DNA polymerase I (Klenow fragment) with a primer−template binds a complementary dNTP and have used this and other fluorescence assays to place the fingers-closing step within the reaction pathway. Because the rate of fingers-closing was substantially faster than the rate of nucleotide incorporation measured in chemical quench experiments, fingers-closing cannot be the rate-limiting prechemistry step defined by earlier kinetic studies. Experiments using Ca^{2+} instead of Mg^{2+} as the metal cofactor suggest instead that the prechemistry step may involve a change in metal ion occupancy at the polymerase active site. The use of ribonucleotide substrates shows there is a base discriminating step that precedes fingers-closing. This earlier step, detected by 2-AP fluorescence, is promoted by complementary nucleotides (ribo- as well as deoxyribo-) but is blocked by mismatches. The complementary rNTP blocks the subsequent fingers-closing step. Thus, discrimination against rNTPs occurs during the transition from open to closed conformations, whereas selection against mismatched bases is initiated earlier in the pathway, in the open complex. Mismatched dNTPs accelerate DNA release from the polymerase, suggesting the existence of an early intermediate in which DNA binding is destabilized relative to the binary complex; this could correspond to a conformation that allows an incoming dNTP to preview the template base. The early kinetic checkpoints identified by this study provide an efficient mechanism for the rejection of mismatched bases and ribose sugars and thus enhance polymerase throughput.

An important characteristic of DNA polymerases is their ability to copy a DNA template with an accuracy far greater than can be accounted for by the thermodynamics of correct versus incorrect base pairs (*1*). The focus of the present study, the Klenow fragment of *E. coli* DNA polymerase I (Pol I(KF)[1]), makes 1 error in $\approx 10^5$ bases copied (*2*). Exonucleolytic proofreading contributes a factor of ≈5-fold to the fidelity of Pol I(KF) (*2*) so that most of the discrimination is provided by recognition processes associated with the polymerase active site. Kinetic studies of a variety of DNA polymerases argue against a mechanism in which discrimination between correct and incorrect base pairs is implemented at a single step, for example, the phosphoryl transfer step where the incoming nucleotide becomes covalently joined to the DNA primer strand. Instead, a sequence of prechemistry steps provide multiple opportunities to reject incorrectly paired substrates, reducing the time spent by the polymerase in processing inappropriate substrates; we refer to these steps as "kinetic checkpoints" (*3*).

The work of Benkovic and co-workers defined the minimal reaction pathway for Pol I(KF) (Scheme 1) using rapid chemical quench methods (*4*). Following the ordered addition of the DNA and dNTP substrates, a key feature of this reaction mechanism is the noncovalent step (step 3) that precedes chemistry (step 4) and is rate-limiting in single-turnover experiments. Kinetic studies of a variety of polymerases, representing different classes (e.g., DNA-dependent or RNA-dependent) and different sequence-homology families, show that the essential features of this pathway are preserved, though there could be differences in the extent to which step 3 or step 4 is rate-limiting (*3, 5*). The prechemistry noncovalent step, or conformational change, was inferred in the Pol I(KF) reaction mechanism because it was rate-limiting, but faster conformational transitions would go undetected in chemical quench experiments. The use of fluorescent probes to report directly on conformational transitions in the reactions of DNA polymerases has provided evidence for additional noncovalent steps between dNTP binding and phosphoryl transfer (*6–15*). These steps are candidates for kinetic checkpoints at which discrimination between complementary and mismatched nucleotides could be implemented.

[†] This work was supported by NIH Grant GM-28550.

* To whom correspondence should be addressed. Catherine M. Joyce, Department of Molecular Biophysics and Biochemistry, Yale University, Bass Center for Molecular and Structural Biology, 266 Whitney Avenue, P.O. Box 208114, New Haven, CT 06520-8114. Phone: (203) 432-8992. Fax: (203) 432-3104. E-mail: catherine.joyce@yale.edu.

[‡] Present address: Novartis Institutes for BioMedical Research, Cambridge, MA 02139.

[§] Present address: Barr Pharmaceuticals, Inc., Northvale, NJ 07647.

[1] Abbreviations: Pol I(KF), Klenow fragment of *E. coli* DNA polymerase I; Klentaq, the portion of *Thermus aquaticus* DNA polymerase equivalent to Klenow fragment; pol, (DNA) polymerase; FRET, fluorescence resonance energy transfer; IAEDANS; 5-(((2-iodoacetyl)amino)ethyl)aminonaphthalene-1-sulfonic acid; TCEP, tris-(2-carboxyethyl)phosphine; 2-AP, 2-aminopurine; DTT, dithiothreitol; dNTP, deoxynucleoside triphosphate.

10.1021/bi7021848 CCC: $40.75
Published on Web 05/13/2008

Scheme 1[a]

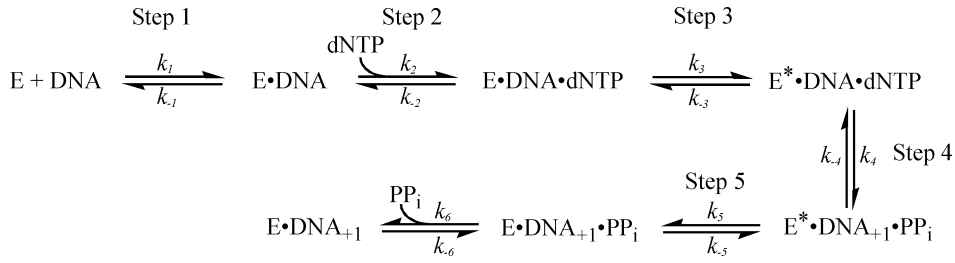

[a] Reprinted with permission from ref 6. Copyright 2003 American Chemical Society.

Cocrystal structures of DNA polymerase complexes identify a prime candidate for a mechanistically important conformational change. Comparing the structures of Pol-DNA binary complexes with the corresponding Pol-DNA-dNTP ternary complexes, there is a substantial movement of a portion of the fingers subdomain while the rest of the protein structure is essentially unchanged (*16–22*). In Pol I(KF), the mobile portion encompasses residues 732 to 766[2] and includes the O-helix, which contains several invariant or highly conserved active-site side chains and is largely responsible for binding the incoming dNTP (*23*). The segmental motion converts the polymerase from an open to a closed conformation in which the newly formed nascent base pair is enveloped by a snug fitting protein surface, providing an obvious method for testing for Watson−Crick complementarity. While it was tempting initially to equate the fingers-closing conformational transition with the noncovalent step 3 of the polymerase reaction pathway (Scheme 1), there was no evidence to support this idea, and more recent studies have suggested that the fingers-closing could be an earlier and more rapid step (*8*). Here, we describe a fluorescence assay in Pol I(KF) that reports the motion of the fingers subdomain, and we use this assay to determine the rate of the fingers-closing transition and deduce its temporal relationship to other steps in the reaction pathway.

EXPERIMENTAL PROCEDURES

Materials. DNA oligonucleotides were synthesized by the Keck Biotechnology Resource Laboratory at Yale Medical School. Oligonucleotides for mutagenesis were used without further purification; those used for kinetics and fluorescence experiments were purified by denaturing gel electrophoresis as described previously (*24*). The reagents for fluorophore labeling, 5-(((2-iodoacetyl)amino)ethyl)aminonaphthalene-1-sulfonic acid (IAEDANS) and tris-(2-carboxyethyl)phosphine (TCEP), were purchased from Molecular Probes (Eugene, OR). Ultrapure dNTPs were purchased from Amersham Biosciences (GE Healthcare).

Construction of Single-Cys Substitutions in Pol I(KF). Mutations encoding single-cysteine substitutions were introduced into a Pol I(KF) expression plasmid using the QuikChange site-directed mutagenesis kit (Stratagene) according to the manufacturer's instructions. The S751C mutation was made for an earlier study (*25*). The Pol I(KF) expression construct, which uses transcriptional and translational signals from phage λ, has been described previously (*26, 27*). The starting plasmid for this study contained the D424A mutation, to inactivate the proofreading 3′−5′ exonuclease (*28*), and C907S, which removes the single cysteine of Pol I(KF) without any detrimental effect on enzymatic activity (*25*). Additionally, to facilitate purification, we used the QuikChange procedure to insert a hexahistidine tag between the first and second amino acids of the KF sequence. For brevity, the N-His_6,D424A,C907S genotype, present in all the proteins in this study, is not listed, and the mutant proteins are described simply by their cysteine substitutions or fluorophore modifications.

Expression and Purification of Pol I(KF) Mutants. Pol I(KF) mutants were expressed in the bacterial host CJ376, as previously described (*26*). The purification method has been changed to benefit from the convenience of metal-chelate affinity chromatography. Cells were suspended in buffer A (50 mM Tris-HCl, pH 8.0, 1 mM 2-mercaptoethanol, 300 mM NaCl) containing 10 mM imidazole, 2 mg/mL lysozyme, and 0.02 mM phenylmethylsulfonyl fluoride, using ≈6.5 mL buffer per g cell paste. The mixture was left on ice for ≈45 min, sonicated to break the cells and reduce the viscosity of the extract, and centrifuged for 25 min at 20,000*g*. The supernatant was batch-equilibrated with Ni-NTA agarose (Qiagen) in buffer A containing 10 mM imidazole, using 4 mL resin per g cell paste, for 1 h at 4 °C. The resin was packed into a column and washed with 10 column volumes of buffer A containing 20 mM imidazole. His-tagged Pol I(KF) derivatives were eluted with 4 column volumes of buffer A containing 100 mM imidazole. Pol I(KF)-containing fractions were pooled and dialyzed into 50 mM Tris-HCl (pH 7.5), 50% (v/v) glycerol, and 0.5 mM dithiothreitol, and stored at −20 °C. Protein concentrations were determined either spectroscopically using $\epsilon_{278} = 63{,}200$ M^{-1} cm^{-1} (*29*) or by SDS−PAGE with quantitation of the Coomassie Blue stained bands relative to a Pol I(KF) standard whose concentration had been measured by quantitative amino acid analysis (Keck Biotechnology Resource Laboratory). Using this expression and purification procedure, a 2 L cell culture yielded ≈3.3 g wet weight of cells and ≈100 mg of highly purified Pol I(KF) derivative.

Labeling of Pol I(KF) Mutants with Fluorophores. Labeling of Pol I(KF) mutants with sulfhydryl-specific fluorescent labels was based on published procedures (*30*). Before labeling, the single-Cys Pol I(KF) mutant protein (200 μL at ≈500 μM) was reduced in the presence of 5 mM DTT at room temperature for 1 h. The mixture was adjusted to ≈200 μM Pol I(KF) and 120 μM TCEP, and was dialyzed against 2 L of 50 mM Tris-HCl (pH 7.5) and 1 mM TCEP, followed by the same buffer containing 120 μM TCEP. The protein

[2] Because the relevant binary and ternary complex cocrystal structures are not available for Pol I(KF), the residue numbers are inferred from structural data from the A-family homologues, T7 DNA polymerase, Klentaq, and Bst DNA polymerase (*17–19*).

concentration after dialysis was estimated spectroscopically, and a 2-fold molar excess of IAEDANS was added. The mixture was incubated overnight at 4 °C with gentle agitation. The reaction was stopped by the addition of DTT to 1 mM. Free fluorophore in solution was removed by extensive dialysis against 50 mM Tris-HCl (pH 7.5), and the labeled protein was further concentrated using a Microcon YM-3 centrifugal concentrator (Millipore). SDS−PAGE fractionation and examination of the gel under UV illumination were used to assess the labeling of the protein and the removal of unbound fluorophore from solution. The extent of labeling was calculated from the UV spectrum, using the extinction coefficient 6100 M^{-1} cm^{-1} at 336 nm for IAEDANS (*31*), and correcting for the contribution of IAEDANS at 278 nm; typically, the Cys side chain was ≥80% labeled. We have demonstrated the specificity of the labeling reaction by showing that the N-His_6,D424A,C907S protein, which contains no Cys side chains, did not become derivatized using a 4-fold molar excess of IAEDANS under the reaction conditions described above.

Chemical Quench Kinetic Measurements. The DNA substrate used in kinetic measurements on the KF derivatives in this study consisted of the 13-mer primer, (5′)GAGTCAACAGGTC(3′), 5′-labeled with ^{32}P, annealed to a 1.5-fold molar excess of the complementary 19-mer (5′)GGTAGXGACCTGTTGACTC(3′), where X, the templating base, was A or C. (The template C version corresponds to the L:unmod sequence shown in Figure 1.) Single-turnover measurements to determine k_{pol} and K_d for addition of the dNTP complementary to the templating base were carried out at room temperature (20−22 °C) using a rapid-quench-flow instrument (KinTek Corp., Model RQF-3) for fast reactions and manual quenching when the reaction was sufficiently slow. The enzyme−DNA solution contained 0.1 μM primer−template duplex and 0.5 μM Pol I(KF) in 50 mM Tris-HCl (pH 7.5) and 10 mM $MgCl_2$. The reaction was initiated by the addition of an equal volume of the appropriate dNTP in the same Tris-$MgCl_2$ solution. Reactions were quenched at the desired time intervals using excess EDTA and were fractionated on denaturing polyacrylamide−urea gels. The data were processed as described previously (*24*). Single-turnover rates were determined at a series of dNTP concentrations and k_{pol} and K_d were determined from a plot of rate versus dNTP concentration fitted to a hyperbolic equation. To determine the amount of active polymerase after fluorophore labeling, analogous kinetic measurements were carried out under burst conditions, with DNA in 2-fold excess over the polymerase. In a typical experiment, the final concentrations in the reaction were 0.5 μM primer−template, 0.25 μM Pol I(KF), and 100 μM dNTP. The amplitude of the initial burst of product formation was used to calculate the concentration of active enzyme (*32*).

Fluorescence Emission Spectra. Steady-state fluorescence spectra were recorded at 22 °C using a Photon Technology International scanning spectrofluorometer. Emission spectra of AEDANS-labeled Pol I(KF) complexes with DNA were measured using solutions containing 1 μM Pol I(KF), 2 μM DNA, 50 mM Tris-HCl (pH 7.5), 5 mM $MgCl_2$, and 1 mM EDTA. Complementary or noncomplementary dNTPs were present as required (see text and Figure legends). AEDANS-labeled samples were excited at 350 nm, and emission spectra were collected from 360 to 650 nm.

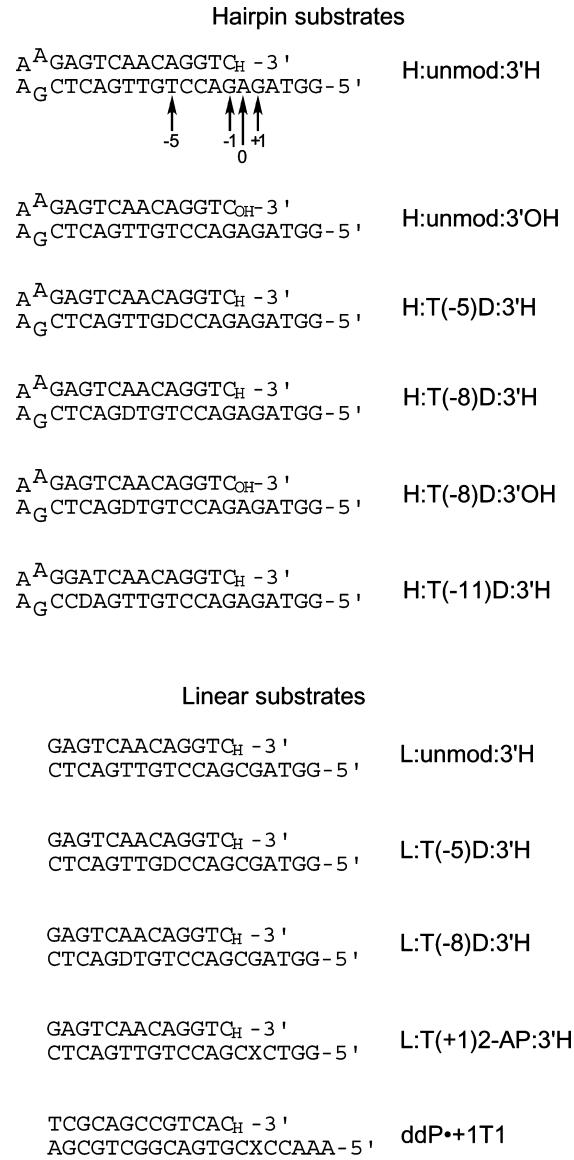

FIGURE 1: DNA oligonucleotides used in this study. Two series of oligonucleotides were designed that employed essentially the same duplex DNA sequence, either as a hairpin with A as the templating base or as a linear duplex with C as the templating base. Within the sequence, dabcyl-dT is shown as D and 2-AP as X. Our numbering convention, relative to the templating position as 0, is shown beneath the first sequence and is used to describe the positions of the dabcyl modifications on the template (T) strand. Dideoxy-terminated primer strands (designated 3′H) were used to trap Pol-DNA-dNTP ternary complexes, and deoxy-terminated primers (designated 3′OH) were used in some experiments to allow covalent addition to the primer terminus. An analogous series of linear 3′OH substrates (not listed) was made by annealing the equivalent deoxy-terminated primer to the template strands illustrated. Chemical quench experiments were carried out using L:unmod:3′OH DNA for incorporation opposite template C and analogous sequences to study incorporation opposite other templating bases. The 2-AP containing ddP•+1T1 duplex, and its extendable counterpart, dP•+1T1, were used in a previous study (*6*).

Stopped-Flow Fluorescence. Stopped-flow experiments were performed at 22 °C using an Applied Photophysics SX.18MV spectrofluorometer. To investigate ternary complex formation by Pol I(KF), one drive syringe contained AEDANS-labeled Pol I(KF) and a nonextendable (dideoxy-terminated) DNA primer−template duplex and the other contained dNTP. Rapid mixing of these two solutions gave final concentrations of 1 μM Pol I(KF), 2 μM DNA, and

varied dNTP concentrations. The buffer in both syringes was 50 mM Tris-HCl (pH 7.5), 1 mM EDTA, and 5 mM of $MgCl_2$ or $CaCl_2$. Using $CaCl_2$ as the metal cofactor permitted ternary complex formation, with no covalent addition to the primer terminus, using an extendable (deoxy-terminated) primer under reaction conditions otherwise identical to those described above. When measuring covalent dNTP incorporation into an extendable primer, the concentrations were as above except that Pol I(KF) was in excess over the DNA duplex: 1.5 μM Pol I(KF) and 1 μM DNA. This ensured that the extension reaction did not require more than one turnover by any polymerase molecule. DNA association rates were measured by mixing 0.1 μM AEDANS-modified Pol I(KF) with 0.2 μM dabcyl-modified DNA, both in 50 mM Tris-HCl (pH 7.5), 1 mM EDTA, and 5 mM $MgCl_2$, and observing the ensuing fluorescence decrease. To measure DNA dissociation, the same reaction buffer was used; one drive syringe contained 0.1 μM AEDANS-modified Pol I(KF) with 0.15 μM of a nonextendable dabcyl-modified DNA, and the other contained 2 μM of an unmodified primer−template DNA such as H:unmod:3′H. On mixing the two solutions, the excess unmodified DNA acts as a trap preventing free Pol I(KF) molecules from reassociating with dabcyl-modified DNA molecules, and the resulting increase in AEDANS fluorescence indicates the rate of dissociation. In some instances, the DNA trap solution also contained dNTPs, as indicated in the text. In all of the above procedures, the excitation wavelength used for AEDANS was 350 nm, and fluorescence emission was detected with a 400 nm long-pass filter. In a few experiments, DNA labeled with 2-AP was used as the fluorophore, with excitation at 310 nm and fluorescence emission detected using a 345 nm long-pass filter. Individual traces were acquired for 10 s using a logarithmic timebase, and averages were typically taken from 5 or more traces. Reaction rates were derived from curve-fitting using either Kaleidagraph (Synergy Software, Reading, PA) or the software provided within the Applied Photophysics stopped-flow program. Kinetic simulation was carried out using KinTek Global Kinetic Explorer (KinTek Corporation, Austin, TX).

RESULTS

Experimental Design. To measure the rate of the open-to-closed conformational transition of Pol I(KF), our strategy used FRET between a donor fluorophore on the mobile portion of the fingers subdomain and an acceptor on the DNA primer−template duplex. We used the nonfluorescent acceptor (quencher) dabcyl, introduced during oligonucleotide synthesis as a substituent at the C5-position of appropriately placed T residues within the template strand (Figure 1). On the basis of cocrystal structural data, formation of the closed ternary complex should decrease the distance between the donor fluorophore and the quencher (Figure 2) and therefore result in a decrease in donor fluorescence whose kinetics report the rate of the fingers-closing transition. Donor fluorescence might also be influenced by a change in the donor environment on going from the open to the closed conformation; such effects will complicate the relationship between fluorescence changes and distance changes. Therefore, our goal was to find a donor position where the observed fluorescence changes were strongly dependent on the presence of the dabcyl quencher on the DNA, implying that the donor fluorescence was reporting donor-to-quencher distance and that other effects were largely excluded. By making the appropriate single-Cys substitutions, we tested several positions on the fingers subdomain for attachment of the donor. Derivatization of position 744 with IAEDANS (as donor fluorophore) gave the desired outcome of a strong fluorescence signal that responded exclusively to donor-to-quencher distance, and, therefore, we will focus largely on experiments conducted with this protein, briefly mentioning corroborative data obtained from other labeling strategies. The Förster distance for the IAEDANS-dabcyl pair is ≈40 Å (*33*), ideal for following the distance changes expected in this experiment (Figure 2).

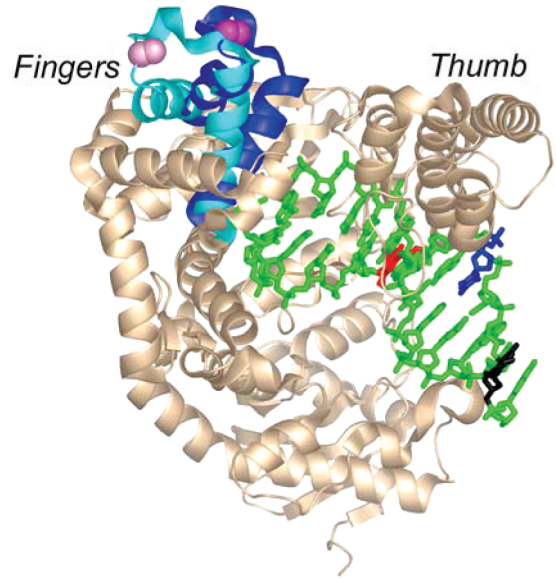

Dabcyl	Distance from 744	
	Open	Closed
T(-11)	59.2	52.8
T(-8)	50.4	43.8
T(-5)	42.9	36.6

FIGURE 2: The fingers-closing conformational change illustrated using structural data from Bst DNA polymerase (*19*). The backbone structure of the binary complex (PDB file 1L3U) is shown predominantly in beige. The chain trace of the ternary complex (PDB file 1LV5) is essentially identical to the binary complex except for the mobile portion of the fingers subdomain, from residues 680 to 714, equivalent to 732 to 766 in Pol I(KF), shown in cyan in the binary complex and blue in the ternary complex. The alpha and beta carbons of residue 692, equivalent to the labeled residue 744 in our study, are shown in spacefilling representation, colored pink and magenta in the binary and ternary complexes, respectively. The DNA primer−template is shown in green; on the template strand, the T(−5), T(−8) and T(−11) positions are colored red, blue, and black, respectively. This illustration was created using PyMOL (DeLano Scientific). The table lists the predicted distances from the beta carbon of Pol I(KF) residue 744 to the template positions at which dabcyl quenchers were attached, measuring to the C5 position of pyrimidines and the C8 position of purines.

Preparation and Characterization of AEDANS-Modified Pol I(KF). Single-Cys substitutions for L744 and other residues in the mobile part of the fingers subdomain were introduced into a 3′−5′ exonuclease-deficient (D424A) Pol I(KF) construct that also had an N-terminal hexahistidine tag, to facilitate purification, and a C907S mutation to eliminate the single Cys of the wild-type protein sequence. Neither of the latter two changes had any significant effect

Table 1: Chemical Quench Data for Pol I(KF) Derivatives Relevant to This Study

protein	reaction[a]	k_{pol} (s^{-1})	K_d (μM)	k_{obs} (s^{-1})[b]	DNA[c]
D424A	A-dTTP	39	11		
His_6,D424A, C907S	A-dTTP	26	12		
Single Cys Mutant: (His_6,D424A,C907S)					
L744C	A-dTTP	39	28		
Modified Cys Mutant: (His_6,D424A,C907S)					
744-AEDANS	A-dTTP	38.0 ± 0.1	26.5 ± 0.9		
744-AEDANS (4 exo^-)[d]	A-dTTP	32	30		
	C-dGTP	46.5 ± 0.7	4.2 ± 0.3	42	
				36	T(−8) dabcyl
				5.5	T(−5) dabcyl

[a] All reactions were carried out under single-turnover conditions (approximately 5:1 E:DNA). Where duplicate measurements were carried out, the results are reported as mean ± s.d. [b] Reaction rate at 50 μM dGTP. [c] DNA substrate was based on the L:unmod sequence (Figure 1) with an extendable (3′OH) primer and with A or C as the templating base, as noted. Where indicated, dabcyl-dT modifications were present. [d] Contained the 3′−5′ exonuclease-deficient mutations D355A, E357A, L361A, and D424A (*34*).

on the Pol I(KF) polymerase reaction (Table 1). A similar L744C construct that was quadruply mutant at the 3′−5′ exonuclease site (D355A,E357A,L361A,D424A)[3] was indistinguishable in its kinetic and fluorescence behavior from the derivative carrying the single D424A exonuclease mutation, arguing against the possibility that any of the observed fluorescence changes might be due to binding of the DNA 3′-end at the exonuclease site. We have used the two exonuclease-deficient constructs interchangeably in the fluorescence experiments described below.

The purified L744C mutant derivative was labeled with IAEDANS, giving 744-AEDANS Pol I(KF). The extent of labeling was typically ≥80%, and the specificity of labeling was demonstrated by the absence of detectable labeling of an equivalent Pol I(KF) construct containing no Cys side chains. On the basis of the fluorescence of appropriately diluted samples on a protein gel, we estimated the amount of nonspecific labeling to be ≤10%. Single-turnover kinetics indicated that neither the L744C mutation nor the 744-AEDANS label were detrimental to the polymerase activity of Pol I(KF) (Table 1). The k_{pol} value was essentially identical for all of the species tested, while the K_d(dNTP) increased slightly with the cysteine substitution. Rapid-quench-flow measurements carried out under burst conditions (E:DNA = 1:2) indicated that the L744C protein was essentially fully active both before and after labeling.

Fluorescence Emission Spectra with Nonextendable DNA Substrates. In order to study conformational transitions that take place before phosphodiester bond formation, the 744-AEDANS Pol I(KF) was bound to a DNA substrate whose primer strand was dideoxy-terminated. Two types of DNA substrates were used (Figure 1): a hairpin structure in which the complementary template and primer strand were linked via a stable tetraloop (*36*) and a linear DNA duplex formed by annealing appropriate template and primer sequences. The templating base was A in the hairpin substrates and C in the annealed linear substrates. Analogous results were obtained with both types of substrates, but we preferred the hairpin substrates because of the very tight binding we have observed with such substrates (*23*) and because they eliminate the possibility of the polymerase binding to the opposite (blunt) end as might occur with the linear substrates. Reaction mixes typically contained 1 μM Pol I(KF) and 2 μM DNA so as to maximize polymerase−DNA binding. Addition of a dNTP to the Pol-DNA binary complex should then form the ternary

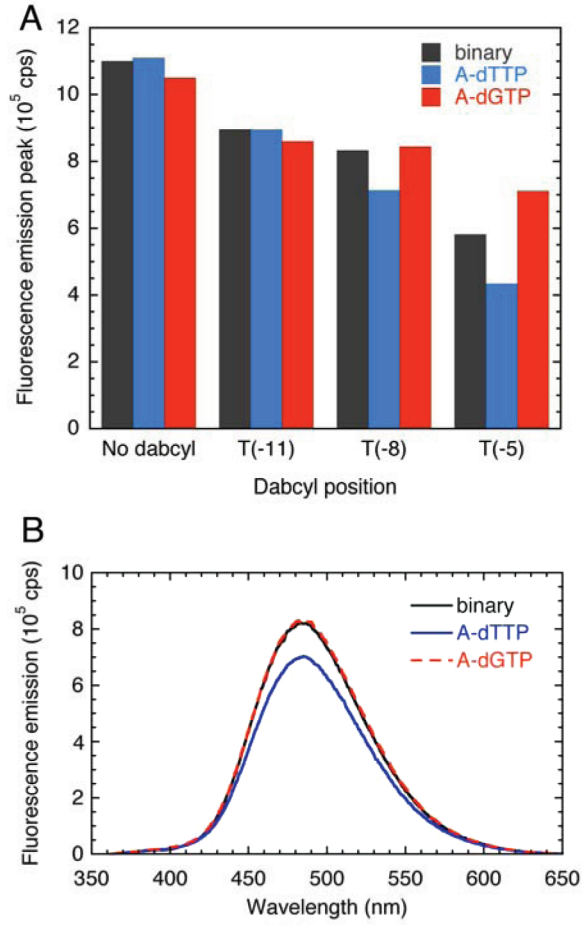

FIGURE 3: Fluorescence emission spectra of 744-AEDANS Pol I(KF) in complex with a series of dabcyl-modified DNA duplexes. The DNAs were from the series of dideoxy-terminated hairpin oligonucleotides illustrated in Figure 1: the control H:unmod:3′H and the dabcyl-modified H:T(−5)D:3′H, H:T(−8)D:3′H, and H:T(−11)D:3′H. These DNAs all had A as the templating base. Spectra were recorded of polymerase and DNA alone (binary complex), and with the addition of the complementary nucleotide dTTP (100 μM) and the mismatched dGTP (500 μM). The bar graph in panel A indicates the fluorescence at the AEDANS emission peak for each sample. Panel B shows an example of the emission spectra with the H:T(−8)D:3′H oligonucleotide.

[3] These mutations eliminate 3 out of the 4 metal ligands and also a side chain (L361) that is one of the most important for DNA binding at the 3′−5′ exonuclease site (*34, 35*).

Table 2: FRET Efficiences in Complexes of 744-AEDANS Pol I(KF) with Dabcyl-Containing DNA Duplexes

	binary, Pol-DNA		ternary, Pol-DNA-dTTP[b]		
DNA[a]	E[c]	R[d]	E	R	ΔR
H:T(−11)D:3′H	0.144 ± 0.033	54.1 ± 2.6	0.169 ± 0.021	52.3 ± 1.3	1.8
H:T(−8)D:3′H	0.160 ± 0.056	53.2 ± 3.3	0.284 ± 0.050	46.8 ± 1.9	6.4
H:T(−5)D:3′H	0.356 ± 0.085	44.4 ± 2.9	0.504 ± 0.073	39.9 ± 2.0	4.5

[a] DNA sequences are listed in Figure 1. [b] The mix contained 100 μM dTTP, complementary to the templating base. [c] FRET efficiency, E, was calculated from fluorescence emission data, such as those shown in Figure 3. Values of E and R were calculated from five independent experiments and are reported as mean ± s.d. [d] The interprobe distance, R, was calculated using 40 Å as the AEDANS-dabcyl Förster distance (*33*).

complex, with the reaction blocked at this point due to the nonextendable primer terminus.

Fluorescence emission spectra demonstrated the effect of the presence and the position of the dabcyl quencher on the AEDANS fluorescence (Figure 3). The AEDANS emission peak in the binary complex (black bars in Figure 3A) was greatest when the DNA had no dabcyl modification and decreased as the dabcyl modification was placed closer to the fingers subdomain, through the series T(−11), T(−8), and T(−5). The presence of dTTP, forming a correctly paired ternary complex (blue bars), had no effect on the AEDANS fluorescence when there was no dabcyl quencher on the DNA, indicating either that ternary complex formation did not significantly change the environment of the 744-AEDANS label or that any environmental change did not translate into an observable change in fluorescence. With the quencher at T(−8) or T(−5), ternary complex formation was associated with a substantial decrease in the AEDANS emission peak (Figure 3A and B), corresponding to formation of the closed conformation which brings donor and acceptor fluorophores closer to one another. With the quencher at T(−11), there was very little change in AEDANS fluorescence associated with dTTP binding, even though the decrease in fluorescence of the binary complex due to the T(−11) quencher suggested that the interprobe distance was sufficiently close to allow FRET. The interprobe distances calculated from the FRET efficiences derived from fluorescence emission spectra (Table 2) were in good agreement with the distances estimated from cocrystal structures (Figure 2), which took no account of the size of the probe molecules and their flexible linker attachments. The emission data for the T(−11) dabcyl quencher agreed least well with the cocrystal predictions; we note that T(−11) is on the opposite side of the DNA helix from T(−8) and T(−5), and this may allow a flexibly attached probe at T(−11) to assume a position more nearly equidistant from the two predicted positions of the side chain at 744, accounting for the unexpectedly small fluorescence change on forming the ternary complex.

Stopped-Flow Fluorescence with Nonextendable DNA Substrates Shows Fingers-Closing Is a Fast Early Step. To determine the rate of the conformational transition that brings donor and acceptor fluorophores closer together, an appropriately labeled Pol-DNA binary complex was mixed in the stopped-flow instrument with the complementary dNTP, and the resulting fluorescence change was recorded. Consistent with the emission spectra results, a binary complex of 744-AEDANS Pol I(KF) with the unmodified DNA hairpin, H:unmod:3′H, gave no change in AEDANS fluorescence when mixed with the correctly paired dTTP, aside from photobleaching at long reaction times (Figure S1 in Supporting Information). With the H:T(−8)D:3′H duplex, containing a dabcyl quencher on the T(−8) base, dTTP addition caused a substantial fluorescence decrease (Figure 4A), which could be fitted to a double exponential followed by a slow linear decay corresponding to photobleaching (see Figure S2 in Supporting Information for an example of curve fitting and residuals). The rates and amplitudes of the fast rate ($Rate_1$) had a hyperbolic dependence on dTTP concentration, with a maximum rate of 120 s^{-1}, and an apparent K_d of 8.4 μM (Figure 4B). $Rate_1$ decreased slightly at dTTP concentrations above 100 μM; possible reasons for this are examined in the Discussion. The slower phase ($Rate_2$) had a rate of ≈20 s^{-1} and an amplitude about one-fourth of that of the fast phase. The stopped-flow kinetic data are summarized in Table 3 and can be compared with the chemical quench data on the same DNA sequence (Table 1). Analogous observations were made using the H:T(−5)D:3′H DNA substrate (Figure 4C and D), except that $Rate_1$ and $Rate_2$ derived from the fluorescence decrease were slower than the corresponding rates with the T(−8) dabcyl DNA, as in the chemical quench experiments (compare Tables 1 and 3).

Stopped-flow fluorescence experiments using the dideoxy-terminated linear DNA substrates L:T(−8)D:3′H and L:T(−5)D:3′H exactly paralleled those described above for the hairpin substrates (Table 3 and Figure S3 in Supporting Information). With C as the templating base in the linear duplexes, the reaction rates were faster than those opposite the template A in the hairpin DNAs. With L:T(−8)D:3′H, a substantial fraction of the fluorescence change at 15 and 25 μM dGTP occurred within the instrument dead time so that the rates of these reactions could not be determined reliably; we have estimated the maximum value of $Rate_1$ to be at least 400 s^{-1}.

Alternative Strategies for Obtaining Ternary Complexes. In the experiments described above, nonextendable (3′H) primers were used in order to stop the polymerase reaction at the formation of the ternary complex. Because the primer 3′OH is an important ligand to one of the active-site metal ions, we explored alternative strategies for blocking the reaction at ternary complex formation. When the noncleavable nucleotide analogue, $\alpha\beta$-imino-dUTP, was used with a normal 3′OH primer in the 744-AEDANS/T(−8)Dabcyl FRET-based assay, we did not observe any fluorescence change on addition of the nucleotide to 100 μM final concentration (data not shown). A more successful strategy was the use of Ca^{2+} instead of Mg^{2+} as the metal ion cofactor. Binding of dTTP to a 744-AEDANS Pol I(KF) binary complex with H:T(−8)D:3′OH in the presence of Ca^{2+} gave a biphasic fluorescence decrease similar to that observed when using H:T(−8)D:3′H in the presence of Mg^{2+} (Figure S4 in Supporting Information). The rate of the first phase ($Rate_1$) was essentially identical with either Ca^{2+}/3′OH or Mg^{2+}/3′H; however, the second phase ($Rate_2$) was about

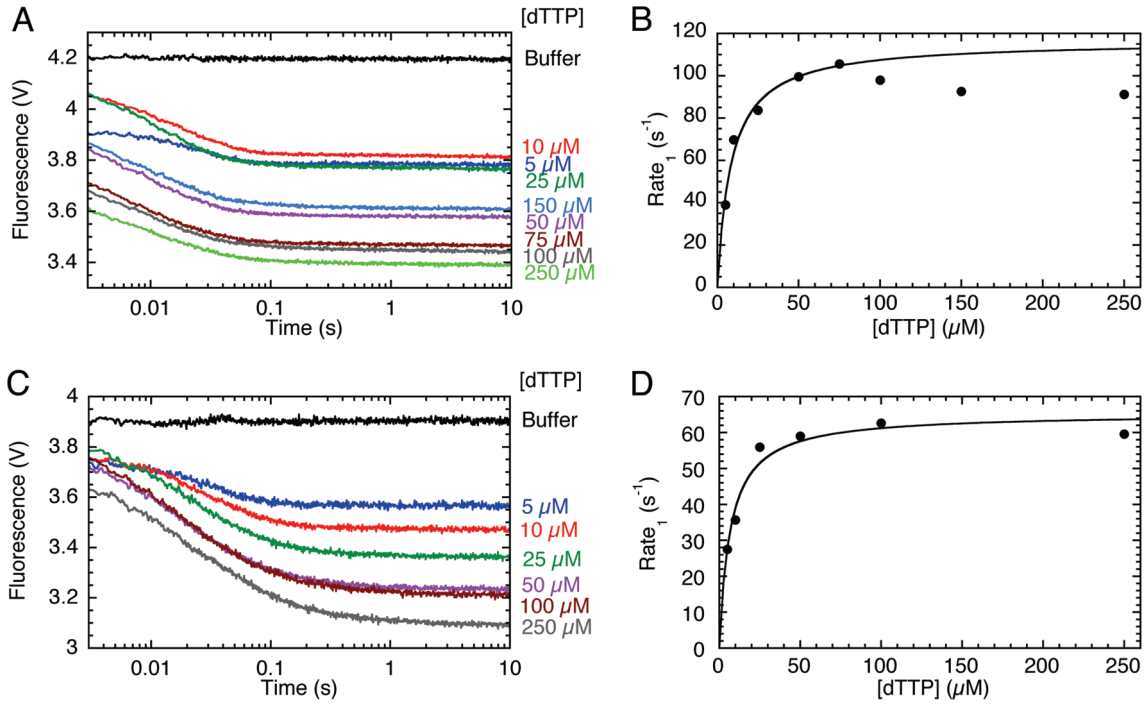

FIGURE 4: Stopped-flow fluorescence study of ternary complex formation using 744-AEDANS Pol I(KF) and nonextendable hairpin DNA duplexes containing dabcyl modifications. In panel A, a binary complex of 744-AEDANS Pol I(KF) with H:T(−8)D:3′H was mixed in the stopped-flow instrument with the complementary nucleotide, dTTP, to give the final concentrations indicated. The data were fitted to a double exponential (as in Figure S2 in Supporting Information) and $Rate_1$ was plotted as a function of dTTP concentration (panel B), giving the results reported in Table 3. Because $Rate_1$ tends to decrease at higher concentrations of nucleotide, the curve fitting in panel B was limited to concentrations up to 75 μM. Panels C and D show an analogous experiment using H:T(−5)D:3′H as the DNA substrate.

Table 3: Reaction Rates Derived from Stopped-Flow Fluorescence Data with 744-AEDANS Pol I(KF)

DNA[a]	reaction[b]	$Rate_1$ (s^{-1})[c]	Amp_1 (V)[c]	$Rate_2$ (s^{-1})[c]	Amp_2 (V)[c]	$Rate_1$ k_{max} (s^{-1})[d]	$K_{d\ app}$ (μM)[d]
H:T(−8)D:3′H	A-dTTP	140 ± 30	0.26 ± 0.04	23 ± 15	0.069 ± 0.034	130 ± 10	11 ± 3
H:T(−5)D:3′H	A-dTTP	64 ± 2	0.31 ± 0.11	9.2 ± 1.2	0.18 ± 0.02	65	6.8
L:T(−8)D:3′H	C-dGTP	320 ± 40	0.32 ± 0.05	46 ± 40	0.044 ± 0.034	>400	
L:T(−5)D:3′H	C-dGTP	110	0.45	7.9	0.16	140	1.6
			Extendable Primer:				
H:T(−8)D:3′OH	A-dTTP	130 ± 20	0.19	26 ± 6	−0.27	110 ± 4 ($Rate_1$) 30 ± 8 ($Rate_2$)	2.5 ±0.1 21 ± 6
			Ca^{2+} as Metal Cofactor:				
H:T(−8)D:3′OH	A-dTTP (Ca^{2+})	95 ± 12	0.20 ± 0.04	3.2 ± 1.8	0.027 ± 0.006	130	24
H:T(−8)D:3′H	A-dTTP (Ca^{2+})	110	0.22	4.0	0.04		
			2-AP Reporter:				
L:T(+1)2-AP:3′H	C-dGTP	220 ± 50	−0.78 ± 0.15	51 ± 3	0.23 ± 0.07	290 ± 60	3.0 ± 0.7

[a] DNA duplex substrates are as illustrated in Figure 1. [b] The metal ion cofactor was Mg^{2+} except for the two experiments indicated, where it was Ca^{2+}. [c] Individual rates and amplitudes are reported for reactions carried out in 100 μM dTTP (hairpin substrates) or 10 μM dGTP (linear substrates). Where multiple measurements were carried out, the results are reported as mean ± s.d. [d] The k_{max} and $K_{d\ app}$ values were derived from rate measurements at a series of dNTP concentrations, as in Figure 4B and D. Unless indicated otherwise, the data apply to $Rate_1$.

7-fold slower in the presence of Ca^{2+} (Table 3). Similar kinetics were observed with Ca^{2+} regardless of the presence of the primer 3′OH (Table 3), implying that 3′H-terminated primers do not compromise the prechemistry steps of the polymerase reaction. Chemical quench experiments, using the same Ca^{2+}-containing buffer conditions, demonstrated extremely slow covalent dNTP addition corresponding to a rate of $\approx 7 \times 10^{-4}$ s^{-1}, 5,000-fold slower than $Rate_2$. Because we did not take special precautions to eliminate Mg^{2+} from the Ca^{2+} experiments, other than including EDTA at 1 mM, the slow incorporation reaction may correspond to catalysis by trace amounts of the natural metal cofactor.

We demonstrated that the early steps of ternary complex formation proceed normally with Ca^{2+} and a 3′OH primer by using wild-type (D424A) Pol I(KF) and a 2-AP(+1) duplex, as in our earlier work (*6*). On addition of the complementary dNTP, the rapid fluorescence increase characteristic of the 2-AP(+1) reporter was observed with Ca^{2+} or Mg^{2+}, but the subsequent decrease, attributed to covalent addition of the nucleotide, was only seen in the presence of Mg^{2+} (Figure S5A in Supporting Information). In the absence of the 3′OH, very similar fluorescence increases were seen with either Ca^{2+} or Mg^{2+} (Figure S5B in Supporting Information). Neither the 2-AP(+1) reporter (Figure S5A

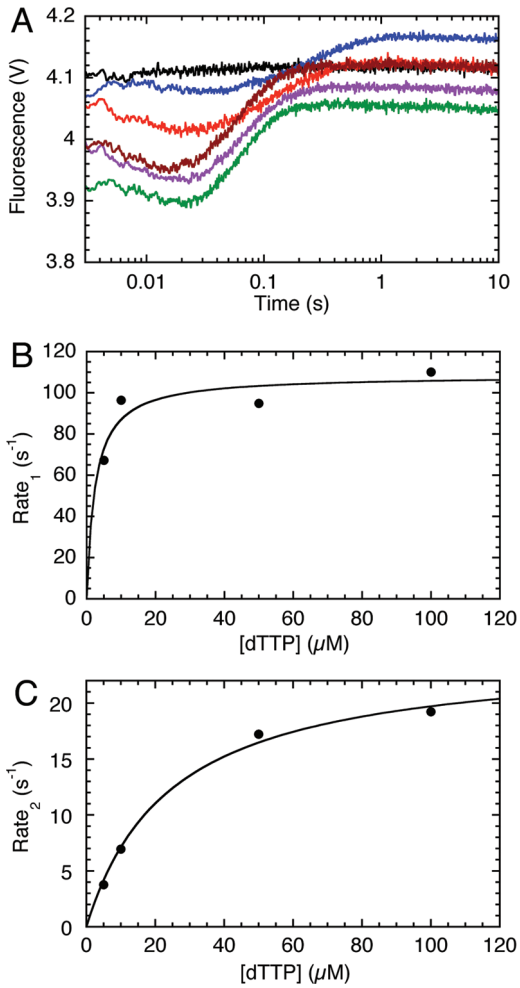

FIGURE 5: Stopped-flow fluorescence study of DNA polymerase-catalyzed addition to an extendable DNA duplex. In panel A, a binary complex of 744-AEDANS Pol I(KF) with H:T(−8)D:3′OH was mixed in the stopped-flow instrument with buffer (black trace) or the complementary nucleotide, dTTP, to give final concentrations of 5 μM (blue), 10 μM (red), 25 μM (green), 50 μM (purple), and 100 μM (brown). The traces were fitted to double exponentials, and Rate$_1$ (panel B) and Rate$_2$ (panel C) were plotted as a function of dTTP concentration, giving the results reported in Table 3. Because of the opposing directions of the two fluorescence changes, it was difficult to extract reliable data from this experiment.

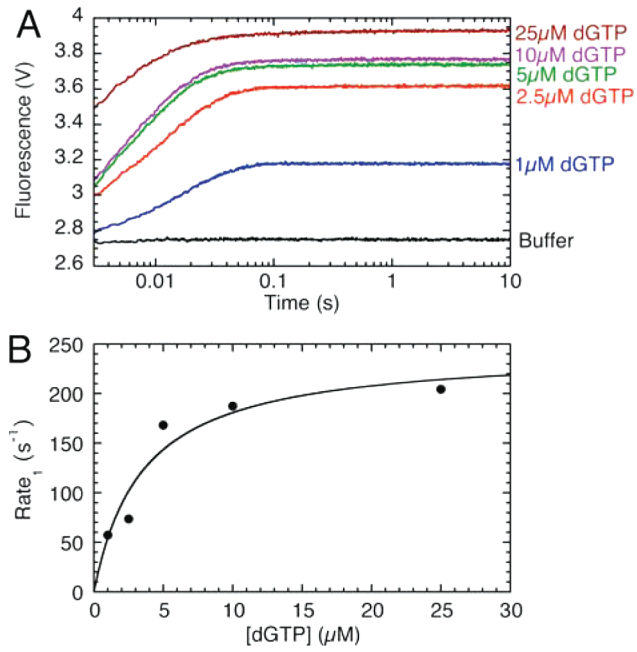

FIGURE 6: Stopped-flow fluorescence study of ternary complex formation using a nonextendable DNA substrate with a T(+1)2-AP reporter. In panel A, a binary complex of the control (N-His$_6$,D424A,C907S) Pol I(KF) (2 μM final concentration) with L:T(+1)2-AP:3′H (1 μM final concentration) was mixed in the stopped-flow instrument with the complementary nucleotide, dGTP, to give the dGTP concentrations indicated. The traces were fitted to double exponentials, and Rate$_1$ was plotted as a function of dGTP concentration (panel B), giving the results reported in Table 3.

in Supporting Information) nor the FRET-based assay (data not shown) gave any fluorescence change in the absence of divalent metal ions.

Further validation of the results obtained with nonextendable DNA primers or unnatural metal cofactors was provided by stopped-flow fluorescence experiments using an extendable, 3′OH-containing, DNA in the presence of Mg^{2+}. When using an extendable DNA, we modified the conditions used in our previous stopped-flow measurements so as to have the 744-AEDANS Pol I(KF) in excess over the DNA (E:DNA = 1.5:1), thus preventing multiple turnovers by a single enzyme molecule on more than one DNA molecule. Using the dabcyl-modified H:T(−8)D:3′OH DNA duplex, a biphasic fluorescence change was observed (Figure 5A). The faster phase (Rate$_1$) was a fluorescence decrease whose rate was similar to Rate$_1$ obtained with the corresponding nonextendable substrate. The rate of the second phase was also similar to the corresponding rate (Rate$_2$) observed with the nonextendable substrate. However, the direction of the change was the opposite (an increase) and the amplitude was greater, consistent with the expectation that covalent addition of dTTP should be followed by either translocation and fingers-opening or dissociation, processes which will increase the distance between 744-AEDANS and the dabcyl quencher. Both Rate$_1$ and Rate$_2$ had a hyperbolic dependence on dTTP concentration, with kinetic parameters in good agreement with those obtained using nonextendable DNA substrates (Figure 5B and C and Table 3).

Stopped-Flow Fluorescence Using a 2-AP Reporter Reveals a Rapid Base-Selective Step Distinct from Fingers-Closing. Because Rate$_1$ measured using 744-AEDANS and the T(−8)dabcyl DNA substrates in the current study was similar to the rate observed previously using 2-AP at the T(+1) position (*6*), we investigated whether the two different fluorophores might be reporting the same process. We designed a DNA substrate based on the L:unmod:3′H sequence, but having 2-AP at the T(+1) position and used this in stopped-flow fluorescence experiments with a nonfluorescent Pol I(KF) (carrying the N-His$_6$,D424A,C907S substitutions). As in our previous study, the 2-AP reporter gave a biphasic fluorescence increase (Figure 6A), whose rates were very similar to those reported previously on a different DNA sequence (*6*). The kinetic parameters obtained with 2-AP were similar in magnitude to those observed with the 744-AEDANS/T(−8)dabcyl system (Figure 6B and Table 3) and therefore did not rule out the possibility that both probes were detecting the same process.

Addition of ribonucleotides proved particularly informative in distinguishing the steps reported by the 2-AP and FRET-based probes (Figure 7). With a T(+1)2-AP reporter, addition of the complementary rGTP caused a rapid fluorescence

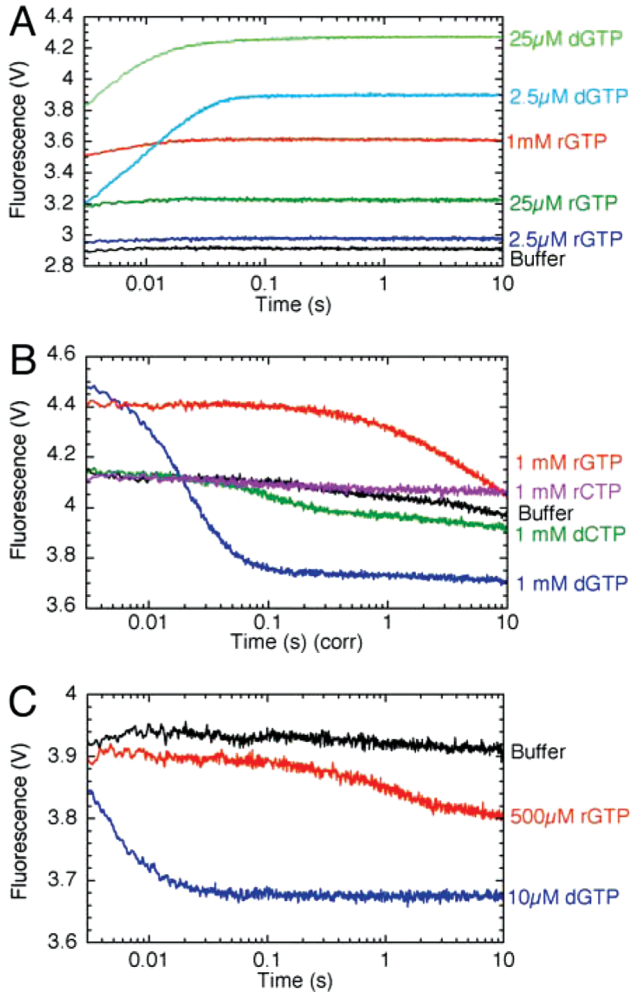

FIGURE 7: Stopped-flow fluorescence study of ribonucleotide addition, comparing a T(+1)2-AP reporter (panels A and B) and the FRET-based 744-AEDANS/T(−8)dabcyl assay. In panel A, the DNA substrate, L:T(+1)2-AP:3′H, had a nonextendable primer terminus and C as the templating base. The binary complex of the control (N-His_6,D424A,C907S) Pol I(KF) (2 μM final concentration) with L:T(+1)2-AP:3′H (1 μM final concentration) was mixed in the stopped-flow instrument with the complementary ribo- or deoxyribonucleotides, to give the final concentrations indicated. In panel B, the extendable substrate dP•+1T1, which also has a template C, was used. The final concentrations of Pol I(KF) and DNA were 0.8 μM and 0.2 μM, respectively, and both complementary (dCTP and rCTP) and mismatched (dGTP and rGTP) nucleotides were tested. The fluorescence decay seen after the addition of dGTP had a rate of 45 s^{-1}, very similar to the chemical quench k_{pol}, 46 s^{-1}, determined for this same DNA substrate in an earlier study (*6*). With rGTP, the fluorescence decay had a rate of 0.28 s^{-1}, and the chemical quench rate was 0.11 s^{-1}. In panel C, 744-AEDANS Pol I(KF) (1 μM final concentration) and L:T(−8)D:3′H (2 μM final concentration) were used, and the slow fluorescence decay observed on addition of rGTP (≈1 s^{-1}) contrasts with the rapid decay on addition of dGTP ($Rate_1$ = 350 s^{-1}; $Rate_2$ = 75 s^{-1}).

increase, much of which took place within the instrument dead time (Figure 7A and B). The fluorescence change was dependent on complementarity (Figure 7B) and was similar to that observed on dGTP addition except that the amplitudes were smaller in rNTP reactions. With an extendable T(+1)2-AP DNA, a fluorescence decrease followed the initial rapid increase, but the rate of this decrease was ≈100-fold slower for rGTP addition compared with dGTP addition (Figure 7B), similar to the published differences in chemical incorporation

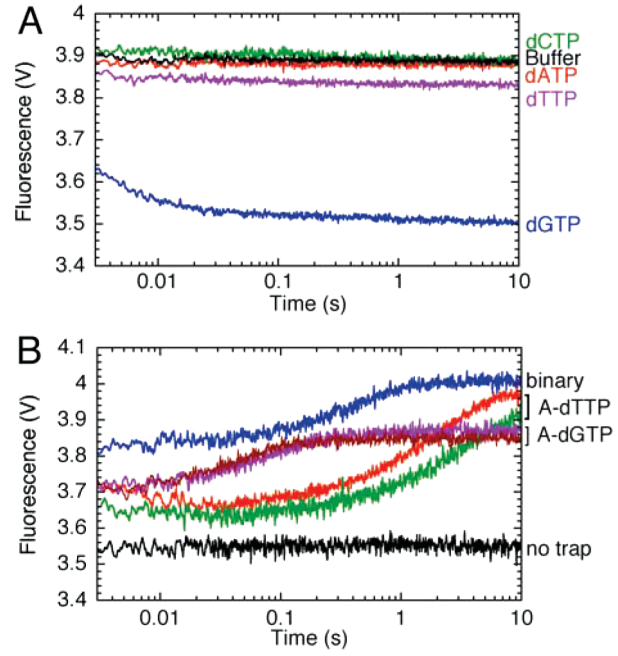

FIGURE 8: Effect of mismatched dNTPs on polymerase−DNA binary complexes. (A) The FRET-based fingers-closing assay. A binary complex of 744-AEDANS Pol I(KF) (1 μM final concentration) with L:T(−8)D:3′H (2 μM final concentration) was mixed in the stopped-flow instrument with reaction buffer, the complementary nucleotide, dGTP (50 μM final concentration), or each mismatched dNTP (500 μM final concentration). (B) The dissociation rate of 744-AEDANS Pol I(KF) from H:T(−8)D:3′H was measured in the stopped-flow instrument by using a DNA trap as described in Experimental Procedures. The black trace is from a control in which the second syringe contained reaction buffer only. The blue trace records dissociation of the binary complex when mixed with the DNA trap. To measure dissociation of the correctly paired ternary complex, the DNA trap solution contained dTTP at 100 μM (red trace) or 500 μM (green trace). To measure dissociation in the presence of a mismatch, the DNA trap solution contained dGTP at 100 μM (purple trace) or 500 μM (brown trace). The dissociation rates are listed in Table 4.

rates for dNTP and rNTP substrates (*37*). Using the FRET-based assay, the complementary rGTP addition did not give any rapid fluorescence changes similar to those seen on dGTP addition; instead there was a very slow fluorescence decrease (≈1 s^{-1}) of smaller amplitude than that obtained with dGTP (Figure 7C). Because the addition of the complementary rNTP had very different effects on the FRET-based and T(+1)2-AP assays, these assays are clearly reporting distinct steps of the reaction.

Noncomplementary dNTPs Preclude Fingers-Closing. Addition of noncomplementary dNTPs to a binary complex of 744-AEDANS Pol I(KF) with a nonextendable T(−8)dabcyl DNA did not cause any change in the fluorescence signal observed in the stopped-flow instrument (Figure 8). Similar observations were made with A or C as the templating base and are consistent with the corresponding emission spectra data for a ternary complex containing a T(−8) dabcyl DNA and an A-dGTP mispair (red bars in Figure 3A and red trace in Figure 3B). In some experiments we have observed a fluorescence increase in response to addition of a mismatched dNTP, exemplified by the emission spectrum using a T(−5) dabcyl DNA (Figure 3A). We believe this fluorescence increase results from dissociation of the quencher-labeled DNA from the complex because its rate is similar to the

Table 4: Rates of Dissociation of Pol I(KF) Complexes with DNA

protein	DNA[a]	dNTP[b]	k_{off} (s^{-1})[c]
744-AEDANS	H:T(−8)D:3′H (A)	none	2.4
		dTTP (100 μM)	0.50
		dTTP (500 μM)	0.31
		dGTP (100 μM)	10
		dGTP (500 μM)	20
751-AEDANS	H:T(−8)D:3′H (A)	none	4.8
		dTTP (100 μM)	1.8
		dTTP (500 μM)	1.3
		dGTP (100 μM)	16
		dGTP (500 μM)	33

[a] The templating base is shown in parentheses. [b] dNTP was present in the syringe with the unmodified trap DNA. [c] Rates were determined by fitting the fluorescence increase to a single exponential.

dissociation rate determined independently (see below). Moreover, the mismatch-dependent fluorescence increase tends to occur in situations favorable to dissociation: lower concentrations of enzyme and DNA or modifications such as T(−5) dabcyl that are somewhat detrimental to binding.

Effects of Complementary and Noncomplementary Nucleotides on DNA Binding. Because the binding of 744-AEDANS Pol I(KF) to a dabcyl-modified DNA duplex causes quenching of the AEDANS fluorophore, this provides a convenient assay for polymerase−DNA association and dissociation. When 744-AEDANS Pol I(KF) and H:T(−8)D:3′H DNA were placed in separate drive syringes in the stopped-flow instrument and mixed to initiate DNA binding, a rapid fluorescence decrease was observed, consistent with a diffusion-limited association rate constant of 10^8 to 10^9 M^{-1} s^{-1} (data not shown). Dissociation was measured by mixing the polymerase−DNA complex, in one drive syringe, with a large excess of unmodified DNA to act as a trap, preventing polymerase molecules, once dissociated, from reassociating with the quencher-containing DNA. The increase in AEDANS fluorescence as the bound dabcyl DNA was replaced by unmodified DNA gave a rate of 2.4 s^{-1} for dissociation of the binary complex. By including appropriate dNTPs in the solution with the DNA trap, we measured the dissociation of DNA from a ternary complex with a correct A-dTTP nascent base pair and in the presence of a mismatched dGTP. Compared to the binary complex, the ternary complex with the correct dNTP had ≈5-fold slower dissociation, whereas the mismatched dNTP destabilized the complex, resulting in ≈5-fold faster dissociation (Figure 8B and Table 4). Similar results were obtained with Pol I(KF) labeled at a different position (751-AEDANS, Table 4) or when using a T(+1)2AP probe to report DNA binding (data not shown).

Corroborative Data from Other Labeling Positions. During the course of this work, we tested a variety of positions for fluorophore attachment to Pol I(KF) (see Figure S6 in Supporting Information). Derivatization of position 751, at the N-terminus of the O-helix, with IAEDANS gave results very similar to those described above for the fluorophore at 744 (data not shown). Modification with IAEDANS of Cys substitutions at 750, 752, or 756 gave probes that reported fluorescence changes having both quencher-dependent and quencher-independent components. As a result, these labeling positions were less satisfactory for generating a signal that could be related unambiguously to movement of the fingers subdomain, and they were not studied in detail. However, they could prove useful as conformationally sensitive fluorophores analogous to the reporter used by Tsai and Johnson in their studies of T7 DNA polymerase (*7*). They also provide a means of assessing whether quenchers attached to the DNA duplex are themselves perturbing the polymerase reaction. This approach is illustrated by stopped-flow fluorescence kinetics using 750-AEDANS Pol I(KF) (Figure S7 in Supporting Information), which support and extend the chemical quench data (Table 1) by showing similar rates with T(−8)dabcyl DNA and the unmodified control duplex, and slower rates with the T(−5) dabcyl modification.

DISCUSSION

Fluorescence Assay for the Fingers-Closing Conformational Change. We have developed a FRET-based assay, using a fluorescently labeled Pol I(KF) and a quencher-containing DNA, that we believe reports the closing of the fingers subdomain on formation of a correctly paired Pol-DNA-dNTP ternary complex. Because the fluorescence change associated with ternary complex formation is observed only in the presence of the quencher, it can be attributed to a change in the distance between the AEDANS fluorophore attached to position 744 and the dabcyl quencher on the DNA duplex. Moreover, the magnitude of the fluorescence change showed a dependence on quencher position that is broadly consistent with the calculated distances between probe attachment points, especially considering that the calculations take no account of the size of the probe molecules. The T(−8) quencher position is the most satisfactory for future studies because it combines a large signal amplitude and a lack of adverse effects on the reaction rate, as judged by both chemical quench data and stopped-flow fluorescence using the conformationally sensitive 750-AEDANS label.

Fingers-Closing Is Fast Relative to Covalent dNTP Incorporation. The fluorescence decrease associated with ternary complex formation is biphasic, consistently fitting better to a double exponential than to a single exponential. We believe the faster of the two phases ($Rate_1$) arises from the fingers-closing process itself because it accounts for the majority of the amplitude (about 80% with the T(−8) quencher) and is not affected by a change in the divalent metal ion cofactor. Moreover, an equivalent process is observed as a rapid initial fluorescence decrease in circumstances when the substrate can be covalently extended (resulting in a subsequent fluorescence increase). The rapid rate of the fluorescence decrease (≈100 to 300 s^{-1}, depending on the substrate) excludes the possibility that the fingers-closing transition corresponds to the rate-limiting prechemistry step (≈30 to 40 s^{-1} with the substrates in the present study). This places the fingers-closing ahead of step 3 in an updated Pol I(KF) reaction pathway (Figure 9). The slower rate ($Rate_2$) is most probably equivalent to step 3 because of the similarity of this rate, when measured with a nonextendable primer, to the chemical quench rate and to $Rate_2$ when the primer is extendable. The equivalence of the two rates means either that step 3 involves a change in interprobe distance or that the process that gives rise to the $Rate_2$ fluorescence change is rate-limited by step 3. The latter scenario provides an attractive explanation of the biphasic

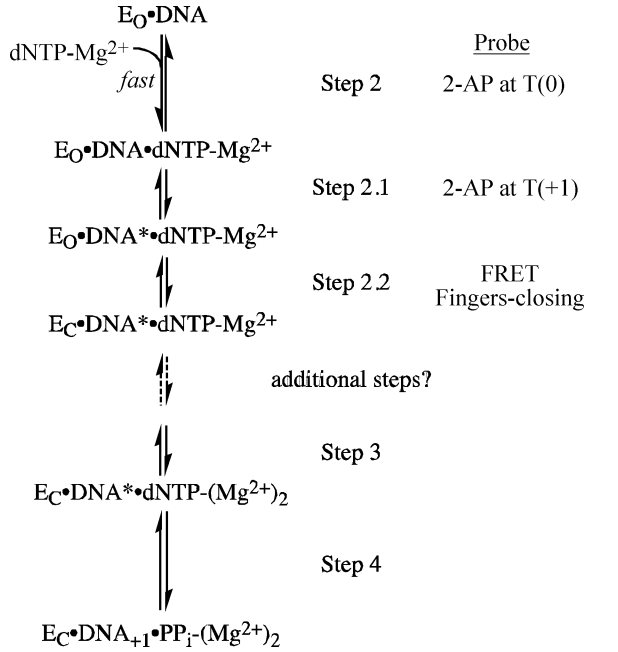

FIGURE 9: Polymerase reaction pathway for Pol I(KF) up to the phosphoryl transfer step. The pathway has been updated to reflect our interpretation of the results in this study. E_O and E_C represent the open and closed conformations of the polymerase. Formation of DNA* in step 2.1 represents the DNA rearrangement that is detected with the T(+1)2-AP probe. For a full explanation of the reasoning supporting this pathway, see the text.

fluorescence change. Using the T(−8) dabcyl complex as an example, the equilibrium across the fingers-closing step would be ≈4:1 in favor of the closed conformation so that the initial conversion to 80% closed complex would be rapid, with subsequent progress toward 100% product being rate-limited by the following slower step. Consistent with this explanation, we note that the relative amplitudes of the fast and slow phases of the FRET assay are influenced by the DNA susbstrate so that, for example, the equilibrium is less favorable to the closed complex with the T(−5) dabcyl substituent (Table 3). An important aspect of the preceding explanation is that it requires only one step of the reaction to be associated with a quencher-dependent fluoresence decrease.

Our experiments demonstrate that fingers-closing is the first step at which significant discrimination against rNTPs takes place. The data of Figure 7C show that a ribonucleotide affects both the rate of fingers-closing and the stability of the closed complex, as shown by the smaller amplitude of the fluorescence change. Destabilization of the closed complex and the preceding transition state by a ribonucleotide would be predicted on structural grounds because the formation of a tight binding pocket will bring the ribose 2′OH into contact with the steric gate side chain (Glu710) (*38*). Rejection of rNTPs via a rapid early step should be beneficial for DNA polymerase efficiency in vivo, where rNTP pools far exceed dNTP pools, by minimizing the time spent processing this unnatural substrate. Complexes with mismatched dNTPs also do not undergo the fingers-closing transition, but we cannot say whether or not the fingers-closing step itself is inhibited by mispairs because it is clear that mismatches will already have been screened out in preceding steps (see below).

Another Fast Recognition Step Precedes Fingers-Closing. The rate of the fingers-closing step is similar to the rate of a process, which we previously designated step 2.1, that is detected using a 2-AP reporter at the T(+1) position (*6*). We believe that step 2.1 may be related to the dislocation of the T(+1) base observed in many polymerase ternary complex crystal structures (*17–19*). The similarity of the two rates suggested that these two processes, fingers-closing and T(+1) rearrangment, might be a single coordinated motion, but this was ruled out by our demonstration that a ribonucleotide substrate had very different effects on the two rates. As described in the previous section, fingers-closing was strongly inhibited by the complementary rNTP. By contrast, the rate of the T(+1) rearrangement was unaffected by the ribonucleotide substitution, suggesting that this step involves a more open conformation in which the ribose 2′OH is out of range of the steric gate side chain. Since, with an rNTP, the T(+1) rearrangement is observed when fingers-closing is strongly inhibited, the T(+1) rearrangement (step 2.1) must precede fingers-closing, and we have therefore placed the fingers-closing as step 2.2 in the updated reaction scheme of Figure 9. Moreover, because the T(+1) rearrangement is blocked by a dNTP (or rNTP) mismatch but not by a complementary rNTP, base discrimination must precede sugar discrimination, implying, most importantly, that a significant element of base discrimination takes place within the open complex.

Polymerase−DNA Binding Is Influenced by Added Nucleotides. We observed that a noncomplementary dNTP accelerates DNA dissociation 5- to 10-fold above the binary complex rate, whereas a correctly paired dNTP decreases the DNA dissociation rate by about 2- to 5-fold (Table 4). Increased stability of the correctly paired ternary complex intuitively makes sense because the conformational equilibrium will be strongly biased toward the closed conformation, but it is less clear why the Pol-DNA interaction is influenced by the presence of a mismatch. Although one might imagine that discrimination could be achieved by having a rapid conformational equilibrium in which the binary complex and mismatched ternary complex populate the closed conformation to different extents, we do not believe that this is the mechanism. As argued above, the sequence of events suggested by our experiments implies that mismatched dNTPs are detected very early in the reaction pathway, before the Pol-DNA complex accesses the closed conformation. Moreover, the fluorescence of the binary complex (in the FRET-based assay) does not increase on addition of a noncomplementary dNTP (Figure 8A)[4], showing that the mismatch does not increase the population of open complexes (and suggesting that binary complexes populate only the open state). This reasoning leads us to conclude that the mismatched dNTP must destabilize the open complex itself and therefore that the dNTP is tested against the templating base within the open complex, perhaps involving an outside-the-pocket base-pairing arrangement similar to that reported in T7 RNA polymerase (*40*), whose polymerase domain structure is extremely similar to that of the A-family DNA polymerases. Making the templating base available for "preview" by the incoming dNTP, as has been discussed in

[4] Two other FRET-based studies report a similar absence of fluorescence changes on addition of mismatched nucleotides (*8, 39*).

earlier publications (*3, 41*), would require a conformational change in the DNA to extract the templating base from its location in the binary complex, a binding pocket at the junction of the O and O1 helices (*19*). If the preview conformation of the DNA template were destabilized relative to the binary complex, this could account for the increased dissociation caused by a mismatch because the mismatched ternary complex would be trapped at this stage. A correctly paired ternary complex, by contrast, would proceed along the reaction pathway and gain increased stability.

Nature of the Rate-Limiting Step 3. Our results rule out the possibility that the slow prechemistry step 3 is the fingers-closing transition, and the experiments using Ca^{2+} suggest an alternative: that step 3 is associated with a change in the metal ion coordination at the active site, perhaps the entry of metal A, which activates the primer 3′OH. There is precedent for this idea in studies of DNA polymerase β, which demonstrated, using exchange-inert dNTP complexes with Cr(III) and Rh(III), that the two active-site metal ions can enter the reaction at different stages (*10, 42, 43*). The metal ion coordinated by the β and γ phosphates is required for dNTP binding, giving a ternary complex that can progress as far as the closed ternary complex in the absence of the second metal ion. Phosphoryl transfer then requires the catalytic metal ion that is coordinated to the primer 3′OH. We assume that the initial binding of the second metal ion is fast and therefore the slow step 3 might involve a subsequent rearrangment of active-site metal ligands, slower with Ca^{2+} than with the canonical Mg^{2+}.

Pol I(KF) Reaction Pathway: Implications for Fidelity. In the updated Pol I(KF) reaction scheme (Figure 9), the fingers-closing conformational transition, step 2.2, follows the two steps that we characterized previously using 2-AP probes. All three of these rapid prechemistry steps have the potential to serve as kinetic checkpoints for the rejection of inappropriate substrates, and, because they are early in the reaction pathway, they improve efficiency by reducing the time that would otherwise be spent processing incorrect substrates. The experiments described here have identified steps at which ribose sugars and incorrectly paired bases are detected. Step 2.2, the fingers-closing step, discriminates against ribonucleotides, probably via simple steric interference as the nucleotide is carried into the active site. Detection of mismatched dNTPs occurs even earlier, somewhere between the entry of the dNTP into the complex (step 2) and the DNA conformational change of step 2.1.

What is the process that provides for screening of noncomplementary nucleotides in the very earliest stages of the DNA polymerase reaction? It is possible that the extremely rapid step 2 encompasses several transitions whose details are obscured in the dead time of the stopped-flow instrument. On the basis of cocrystal structures, one could envisage the Pol-DNA binary complex, with the templating base in the pocket between helices O and O_1, binding an incoming dNTP-Mg^{2+}, initially using contacts between the phosphates and conserved positively charged side chains on the O-helix, as seen in Pol-dNTP complexes (*44, 45*). Movement of the templating base out of the pocket, so as to test complementarity with the incoming dNTP, might generate a structure analogous to that observed in T7 RNA polymerase (*40*) and might also cause the change in the environment of the templating base that accounts for the signal observed with the T(0) 2-AP probe (*6*). With a correct template-dNTP pair, two rapid steps ensue: a further rearrangment of the DNA that exposes the T(+1) base (step 2.1), quickly followed by fingers-closing (step 2.2) in which the movement of the O-helix carries the nascent base pair into the active-site pocket. If a mismatch is identified at step 2, the complex does not normally proceed to step 2.1 but instead follows a different pathway leading to dissociation of the dNTP or the entire Pol-DNA complex. It is unclear whether rare misincorporation events result from the infrequent formation of closed mispair complexes or from inefficient phosphoryl transfer in an improperly aligned open complex.

Comparison with Other Fluorescence Studies of A-Family Polymerases. Two published studies, one of Pol I(KF) and one of Klentaq, are similar to ours, in that they used FRET probes designed to report distance changes. Stengel et al. (*39*) tracked the fingers-closing transition in Pol I(KF) using a fluorescent base analogue adjacent to the primer terminus and an acceptor attached to position 751. Unfortunately, the fluorophores reduced the rate of fingers-closing to the point that it became rate-limiting for polymerase-catalyzed incorporation so that, by the authors' own admission, their experiment does not address the rate of fingers-closing in a more normal situation.

In the FRET-based study of Klentaq by Rothwell et al. (*8*), donor and acceptor fluorophores were attached to residue 649, equivalent to 744 of Pol I(KF), and to the DNA primer strand. Like us, Rothwell et al. concluded that the fingers-closing conformational change is faster than the chemical quench rate. A significant difference, however, is that both rates extracted from the biphasic fluorescence change observed with Klentaq (62 and 20 s^{-1} at 40 °C) were substantially faster than the rate of covalent dNTP addition (0.92 s^{-1} at the same temperature), whereas with Pol I(KF) the slower rate of the fluorescence change is similar to the rate-limiting step that precedes phosphoryl transfer. Because there are no published data establishing the identity of the rate-limiting step in the Klentaq reaction pathway, a possible explanation of the difference between the Pol I(KF) and Klentaq data is that phosphoryl transfer may be rate-limiting for Klentaq. If so, we can interpret the Klentaq data as follows: the biphasic fluorescence change, as in Pol I(KF), would reflect contributions from the fingers-closing step (62 s^{-1}) and from a noncovalent step (20 s^{-1}), equivalent to step 3 in Scheme 1, that precedes a much slower rate-limiting chemical step (0.92 s^{-1}).

Two studies of another A-family homologue, T7 DNA polymerase, both used single conformationally sensitive fluorophores, rather than a FRET pair designed to report distance changes (*7, 46*). The results obtained in these two studies were strikingly different from each other, implying that the two probes report different steps of the reaction. Tsai and Johnson, using a probe attached to the mobile portion of the fingers subdomain, observed a rate of 660 s^{-1} in their fluorescence assay, compared with 230 s^{-1} for the rate of incorporation observed by chemical quench (*7*). Allowing for the faster overall reaction rate of T7 DNA polymerase compared with Pol I(KF), the results of Tsai and Johnson parallel our conclusions that the fingers-closing transition is about 3-fold faster than the rate-limiting step for chemical incorporation. It therefore seems reasonable that the conformationally sensitive probe attached to position 514 of T7

Scheme 2

$$E \bullet DNA_X \xleftrightarrow{slow} E \bullet DNA_0 \xleftrightarrow{+\,dNTP} E \bullet DNA \bullet dNTP \xleftrightarrow{fast} [E \bullet DNA \bullet dNTP]_{closed}$$

DNA polymerase does indeed report the fingers-closing step, consistent with our observations using the equivalent labeling position, 750, in Pol I(KF). A second study of T7 DNA polymerase, using a combination of single-molecule and rapid time scale ensemble measurements with a fluorescent probe attached to the uncopied portion of the DNA template, reported a much faster fluorescence change of 4500 s^{-1} (compared with a chemical incorporation rate of 300 s^{-1}) (*46*). Conceivably, this probe might report a step equivalent to one of the faster steps that precede fingers-closing in our proposed reaction pathway. However, because neither of the T7 DNA polymerase studies demonstrated that the fluorescence signal reports the position of the fingers subdomain, it is impossible to say with certainty which (if any) has targeted the fingers-closing step.

Evaluation of Evidence for a Second Pol-DNA Binary Complex. Recently Rothwell and Waksman have extended their FRET-based study of Klentaq and, on the basis of their results, propose the existence of two forms of Pol-DNA binary complex, which interconvert slowly in comparison with the fingers-closing process (*41*). This inference was made because the fingers-closing rate showed an unusual inverse dependence on the concentration of the complementary dNTP, being fastest at low dNTP concentrations. According to the analysis of Fersht and Requena (*47*), this kinetic behavior can be attributed to the pathway of Scheme 2, which shows two binary complexes, only one of which is able to bind dNTP and generate the fluorescence change corresponding to the fingers-closing process. The slow isomerization of E-DNA_x to the binding-competent E-DNA_0 accounts for the unusual concentration dependence of the observed rate. (Binary complex species that interconvert rapidly are, of course, kinetically silent, behaving as a single kinetic species even though they might be mechanistically distinct.)

We have noted a tendency of the Pol I(KF) fingers-closing rate to decrease at high dNTP concentrations, although the usual increasing hyperbolic concentration dependence is observed at lower concentrations, spanning the K_d determined from chemical quench experiments (see, e.g., Figure 4B). One could argue that this arises from mixed kinetics, with dNTP binding limiting the rate of fingers-closing at low dNTP concentrations, while isomerization of a putative E-DNA_x complex is rate-limiting at high concentrations. However, we have been unable to reproduce the trend seen in Figure 4B by kinetic simulation using a wide range of rate and equilibrium constants for the processes in Scheme 2. Furthermore, Scheme 2 predicts that, when E-DNA isomerization is rate-limiting, an additional faster transition should be observed because of the equilibrium concentration of E-DNA_0 initally present in the reaction mixture. We do not observe this additional faster rate in our data at high dNTP concentrations. It is unclear whether this faster rate is present in the Klentaq data (*41*), even though kinetic simulation using the published rate constants from this study suggests that it should be easily detectable. An alternative interpretation would be that $Rate_1$ observed in our experiments corresponds to the reaction of E-DNA_0, while $Rate_2$ corresponds to the slow conversion of E-DNA_x. In this case, it would be $Rate_2$ that would be expected to decrease with increasing dNTP concentration, a prediction that is difficult to evaluate critically because $Rate_2$ is poorly determined on account of its small amplitude. Therefore, although our data do not rule out the possibility of a second Pol-DNA binary complex, they provide no evidence in favor of the inclusion of such a complex in our reaction schemes. We suspect that the gradual decrease we have observed in the rate of the fluorescence change at high dNTP concentrations ($\geq$10-fold above the apparent K_d) may be caused by inhibition due to high concentrations of nucleotide[5] or may simply be a numerical consequence of the smaller fluorescence amplitudes obtained at high dNTP concentrations (Figure 4A and C).

It is, of course, entirely possible that Pol I(KF) and Klentaq may show different kinetic behavior, attributable to different relative rates of individual steps of the reaction pathway. In the case of Klentaq, slow interconversion of the proposed binary complex species would dominate the kinetics of the fingers-closing fluorescence change, and might be a consequence of the experiments being conducted at a temperature substantially below the optimum for this thermophilic polymerase. For Pol I(KF), different forms of the binary complex may also exist, but, if their interconversion is fast, they will behave as a single kinetic entity.

[5] The trend of Figure 4B can be simulated quite easily by including a dNTP-induced inhibition with a high K_d(dNTP).

ACKNOWLEDGMENT

We are grateful to Enrique De La Cruz and Anna M. Pyle for the use of their stopped-flow instruments.

SUPPORTING INFORMATION AVAILABLE

Additional stopped-flow fluorescence data is presented in Figures S1−S5, and S7. Figure S6 indicates the location of other fluorophore attachment positions that were tested. This material is available free of charge via the Internet at http://pubs.acs.org.

REFERENCES

1. Kunkel, T. A., and Bebenek, K. (2000) DNA replication fidelity. *Annu. Rev. Biochem. 69*, 497–529.
2. Bebenek, K., Joyce, C. M., Fitzgerald, M. P., and Kunkel, T. A. (1990) The fidelity of DNA synthesis catalyzed by derivatives of *Escherichia coli* DNA polymerase I. *J. Biol. Chem. 265*, 13878–13887.
3. Joyce, C. M., and Benkovic, S. J. (2004) DNA polymerase fidelity: kinetics, structure, and checkpoints. *Biochemistry 43*, 14317–14324.
4. Dahlberg, M. E., and Benkovic, S. J. (1991) Kinetic mechanism of DNA polymerase I (Klenow fragment): identification of a second conformational change and evaluation of the internal equilibrium constant. *Biochemistry 30*, 4835–4843.
5. Castro, C., Smidansky, E., Maksimchuk, K. R., Arnold, J. J., Korneeva, V. S., Götte, M., Konigsberg, W., and Cameron, C. E. (2007) Two proton transfers in the transition state for nucleotidyl transfer catalyzed by RNA- and DNA-dependent RNA and DNA polymerases. *Proc. Natl. Acad. Sci. U.S.A. 104*, 4267–4272.
6. Purohit, V., Grindley, N. D. F., and Joyce, C. M. (2003) Use of 2-aminopurine fluorescence to examine conformational changes

during nucleotide incorporation by DNA polymerase I (Klenow fragment). *Biochemistry 42*, 10200–10211.
7. Tsai, Y.-C., and Johnson, K. A. (2006) A new paradigm for DNA polymerase specificity. *Biochemistry 45*, 9675–9687.
8. Rothwell, P. J., Mitaksov, V., and Waksman, G. (2005) Motions of the fingers subdomain of Klentaq1 are fast and not rate limiting: implications for the molecular basis of fidelity in DNA polymerases. *Mol. Cell 19*, 345–355.
9. Shah, A. M., Li, S.-X., Anderson, K. S., and Sweasy, J. B. (2001) Y265H mutator mutant of DNA polymerase β. Proper geometric alignment is critical for fidelity. *J. Biol. Chem. 276*, 10824–10831.
10. Arndt, J. W., Gong, W., Zhong, X., Showalter, A. K., Liu, J., Dunlap, C. A., Lin, Z., Paxson, C., Tsai, M.-D., and Chan, M. K. (2001) Insight into the catalytic mechanism of DNA polymerase β: structures of intermediate complexes. *Biochemistry 40*, 5368–5375.
11. Dunlap, C. A., and Tsai, M.-D. (2002) Use of 2-aminopurine and tryptophan fluorescence as probes in kinetic analyses of DNA polymerase β. *Biochemistry 41*, 11226–11235.
12. Fidalgo da Silva, E., Mandal, S. S., and Reha-Krantz, L. J. (2002) Using 2-aminopurine fluorescence to measure incorporation of incorrect nucleotides by wild type and mutant bacteriophage T4 DNA polymerases. *J. Biol. Chem. 277*, 40640–40649.
13. Hariharan, C., Bloom, L. B., Helquist, S. A., Kool, E. T., and Reha-Krantz, L. J. (2006) Dynamics of nucleotide incorporation: snapshots revealed by 2-aminopurine fluorescence studies. *Biochemistry 45*, 2836–2844.
14. Zhang, H., Cao, W., Zakharova, E., Konigsberg, W., and De La Cruz, E. M. (2007) Fluorescence of 2-aminopurine reveals rapid conformational changes in the RB69 DNA polymerase-primer/template complexes upon binding and incorporation of matched deoxynucleoside triphosphates. *Nucleic Acids Res. 35*, 6052–6062.
15. DeLucia, A. M., Grindley, N. D. F., and Joyce, C. M. (2007) Conformational changes during normal and error-prone incorporation of nucleotides by a Y-family DNA polymerase detected by 2-aminopurine fluorescence. *Biochemistry 46*, 10790–10803.
16. Doublié, S., Sawaya, M. R., and Ellenberger, T. (1999) An open and closed case for all polymerases. *Structure 7*, R31−R35.
17. Doublié, S., Tabor, S., Long, A., Richardson, C. C., and Ellenberger, T. (1998) Crystal structure of a bacteriophage T7 DNA replication complex at 2.2 Å resolution. *Nature 391*, 251–258.
18. Li, Y., Korolev, S., and Waksman, G. (1998) Crystal structures of open and closed forms of binary and ternary complexes of *Thermus aquaticus* DNA polymerase I: structural basis for nucleotide incorporation. *EMBO J. 17*, 7514–7525.
19. Johnson, S. J., Taylor, J. S., and Beese, L. S. (2003) Processive DNA synthesis observed in a polymerase crystal suggests a mechanism for the prevention of frameshift mutations. *Proc. Natl. Acad. Sci. U.S.A. 100*, 3895–3900.
20. Franklin, M. C., Wang, J., and Steitz, T. A. (2001) Structure of the replicating complex of a pol α family DNA polymerase. *Cell 105*, 657–667.
21. Sawaya, M. R., Prasad, R., Wilson, S. H., Kraut, J., and Pelletier, H. (1997) Crystal structures of human DNA polymerase β complexed with gapped and nicked DNA: evidence for an induced fit mechanism. *Biochemistry 36*, 11205–11215.
22. Huang, H., Chopra, R., Verdine, G. L., and Harrison, S. C. (1998) Structure of a covalently trapped catalytic complex of HIV-1 reverse transcriptase: implications for drug resistance. *Science 282*, 1669–1675.
23. Astatke, M., Grindley, N. D. F., and Joyce, C. M. (1995) Deoxynucleoside triphosphate and pyrophosphate binding sites in the catalytically competent ternary complex for the polymerase reaction catalyzed by DNA polymerase I (Klenow fragment). *J. Biol. Chem. 270* 1945–1954.
24. Astatke, M., Grindley, N. D. F., and Joyce, C. M. (1998) How *E. coli* DNA polymerase I (Klenow fragment) distinguishes between deoxy- and dideoxynucleotides. *J. Mol. Biol. 278*, 147–165.
25. Furey, W. S., Joyce, C. M., Osborne, M. A., Klenerman, D., Peliska, J. A., and Balasubramanian, S. (1998) Use of fluorescence resonance energy transfer to investigate the conformation of DNA substrates bound to the Klenow fragment. *Biochemistry 37*, 2979–2990.
26. Joyce, C. M., and Derbyshire, V. (1995) Purification of *E. coli* DNA polymerase I and Klenow fragment. *Methods Enzymol. 262*, 3–13.
27. Polesky, A. H., Steitz, T. A., Grindley, N. D. F., and Joyce, C. M. (1990) Identification of residues critical for the polymerase activity of the Klenow fragment of DNA polymerase I from *Escherichia coli*. *J. Biol. Chem. 265*, 14579–14591.
28. Derbyshire, V., Freemont, P. S., Sanderson, M. R., Beese, L., Friedman, J. M., Joyce, C. M., and Steitz, T. A. (1988) Genetic and crystallographic studies of the 3′,5′-exonucleolytic site of DNA polymerase I. *Science 240*, 199–201.
29. Setlow, P., Brutlag, D., and Kornberg, A. (1972) Deoxyribonucleic acid polymerase: two distinct enzymes in one polypeptide. I. A proteolytic fragment containing the polymerase and 3′−5′ exonuclease functions. *J. Biol. Chem. 247*, 224–231.
30. Haugland, R. P. (2005) *The Handbook: A Guide to Fluorescent Probes and Labeling Technologies*, 10th ed., Invitrogen Corporation, Carlsbad, CA.
31. Hudson, E. N., and Weber, G. (1973) Synthesis and characterization of two fluorescent sulfhydryl reagents. *Biochemistry 12*, 4154–4161.
32. Johnson, K. A. (1995) Rapid quench kinetic analysis of polymerases, adenosinetriphosphatases, and enzyme intermediates. *Methods Enzymol. 249*, 38–61.
33. Wu, P. G., and Brand, L. (1994) Resonance energy transfer: methods and applications. *Anal. Biochem. 218*, 1–13.
34. Derbyshire, V., Grindley, N. D. F., and Joyce, C. M. (1991) The 3′−5′ exonuclease of DNA polymerase I of *Escherichia coli*: contribution of each amino acid at the active site to the reaction. *EMBO J. 10*, 17–24.
35. Lam, W. C., Van der Schans, E. J., Joyce, C. M., and Millar, D. P. (1998) Effects of mutations on the partitioning of DNA substrates between the polymerase and 3′−5′ exonuclease sites of DNA polymerase I (Klenow fragment). *Biochemistry 37*, 1513–1522.
36. Antao, V. P., and Tinoco, I., Jr. (1992) Thermodynamic parameters for loop formation in RNA and DNA hairpin tetraloops. *Nucleic Acids Res. 20*, 819–824.
37. DeLucia, A. M., Chaudhuri, S., Potapova, O., Grindley, N. D. F., and Joyce, C. M. (2006) The properties of steric gate mutants reveal different constraints within the active sites of Y-family and A-family DNA polymerases. *J. Biol. Chem. 281*, 27286–27291.
38. Astatke, M., Ng, K., Grindley, N. D. F., and Joyce, C. M. (1998) A single side chain prevents *Escherichia coli* DNA polymerase I (Klenow fragment) from incorporating ribonucleotides. *Proc. Natl. Acad. Sci. U.S.A. 95*, 3402–3407.
39. Stengel, G., Gill, J. P., Sandin, P., Wilhelmsson, L. M., Albinsson, B., Norden, B., and Millar, D. (2007) Conformational dynamics of DNA polymerase probed with a novel fluorescent DNA base analogue. *Biochemistry 46*, 12289–12297.
40. Temiakov, D., Patlan, V., Anikin, M., McAllister, W. T., Yokoyama, S., and Vassylyev, D. G. (2004) Structural basis for substrate selection by T7 RNA polymerase. *Cell 116*, 381–391.
41. Rothwell, P. J., and Waksman, G. (2007) A pre-equilibrium before nucleotide binding limits fingers subdomain closure by Klentaq1. *J. Biol. Chem. 282*, 28884–28892.
42. Zhong, X., Patel, S. S., and Tsai, M.-D. (1998) DNA polymerase β. 5. Dissecting the functional roles of the two metal ions with Cr(III)dTTP. *J. Am. Chem. Soc. 120*, 235–236.
43. Bakhtina, M., Lee, S., Wang, Y., Dunlap, C., Lamarche, B., and Tsai, M.-D. (2005) Use of viscogens, dNTPαS, and rhodium(III) as probes in stopped-flow experiments to obtain new evidence for the mechanism of catalysis by DNA polymerase β. *Biochemistry 44*, 5177–5187.
44. Beese, L. S., Friedman, J. M., and Steitz, T. A. (1993) Crystal structures of the Klenow fragment of DNA polymerase I complexed with deoxynucleoside triphosphate and pyrophosphate. *Biochemistry 32*, 14095–14101.
45. Li, Y., Kong, Y., Korolev, S., and Waksman, G. (1998) Crystal structures of the Klenow fragment of *Thermus aquaticus* DNA polymerase I complexed with deoxyribonucleoside triphosphates. *Protein Sci. 7*, 1116–1123.
46. Luo, G., Wang, M., Konigsberg, W. H., and Xie, X. S. (2007) Single-molecule and ensemble fluorescence assays for a functionally important conformational change in T7 DNA polymerase. *Proc. Natl. Acad. Sci. U.S.A. 104*, 12610–12615.
47. Fersht, A. R., and Requena, Y. (1971) Equilibrium and rate constants for the interconversion of two conformations of α-chymotrypsin. The existence of a catalytically inactive conformation at neutral pH. *J. Mol. Biol. 60*, 279–290.

BI7021848